

Biochar versus Iron Oxide-biochar Performance as Adsorbents for Lead and Methyl Orange from an Aqueous Solution

Tobias T. Shumba^{1*}, Masimba Tapera^{2,3} and Janety Mumbi³

¹Department of B-Tech, Science Technology Division, Harare Polytechnic, P.O.Box CY 407, Causeway, Harare, Zimbabwe.

²Department of Physical Science, Science Technology Division, Harare Polytechnic, P.O.Box CY 407, Causeway, Harare, Zimbabwe.

³Department of Chemistry, School of Pure and Applied Sciences, Kenyatta University, P.O.Box 43844-00100, Nairobi, Kenya.

Authors' contributions

This work was carried out in collaboration among all authors. All authors read and approved the final manuscript.

Article Information

Editor(s):

(1) Dr. Yang Qu, Associate Professor, Key Laboratory of Functional Inorganic Material Chemistry, Ministry of Education of the People's Republic of China, Heilongjiang University, China.

Reviewers:

(1) Donatus Dube, National University of Science and Technology, Zimbabwe.
(2) Chadetrik Rout, Maharishi Markandeshwar (Deemed to be University), India.
Complete Peer review History: <http://www.sdiarticle4.com/review-history/52734>

Original Research Article

Received 05 September 2019
Accepted 18 November 2019
Published 23 November 2019

ABSTRACT

Water purification is slowly becoming a problem worldwide due to population growth. Lack of proper wastewater disposal from domestic and industrial sources has escalated water pollution in developing countries. Continuous pollution of water sources has made water purification for domestic supplies very expensive. Modern and cost-effective ways of water purification are urgently needed. One of the modern emerging technologies is adsorption using nano-materials. The aim of the study was to prepare an engineered iron oxide-biochar (Fe₂O₃-BC), a nano-composite using pyrolysis and microwave activation. The efficiency of the nano-composite was evaluated in the removal of the heavy metal lead (Pb) and the dye methyl orange (MO) in aqueous solutions. Infrared spectroscopy was used to identify the functional groups present in the synthesized biochars before and after adsorption. The adsorption properties of the synthesised

Fe₂O₃-BC and biochar (BC) were determined by application in lead metal and methyl orange aqueous solutions on known concentrations. FAAS and UV/VIS Spectrophotometry were used for Lead and Methyl Orange concentrations measurements respectively. Batch adsorption experiments were conducted to investigate the capacity of Fe₂O₃-BC and BC to remove MO and Pb in aqueous solutions. A dose of 50 mg Fe₂O₃-BC had the highest percentage MO removal of 89.81% at pH 2 while 50 mg of BC had a highest of 11.55% at pH 12. A dosage of 100 mg of Fe₂O₃-BC had 100% MO removal and 250 mg BC achieved a maximum of 30.61% removal in 30 minutes. Maximum MO removal concentrations were 70 mg/L and 55 mg/L respectively for Fe₂O₃-BC and BC adsorbents. Both Fe₂O₃-BC and BC had Pb²⁺ removal of 97% in 30 minutes. A dose of 65 mg for both Fe₂O₃-BC and BC adsorbents had 100% removal of Pb²⁺. The adsorption studies of both MO dye and Pb²⁺ on Fe₂O₃-BC nano-composite fit the Langmuir isotherm (R² value of 0.999) and Temkin isotherm (R² value of 0.919). The Fe₂O₃-BC nano-composite adsorbs Pb and MO dye better than biochar. The Fe₂O₃-BC nano-composite could be a good adsorbent for other cations and anions. More work need to be done in order to investigate the adsorption potential of other cations and anions using Fe₂O₃-BC nano-composite.

Keywords: Biochar; adsorption; adsorbate; pyrolysis; heavy metal; biosorption.

1. INTRODUCTION

Wastewaters are produced in many industrial processes, mostly from mining, steel mills, tanning plants, production of chemical fertilizers and pesticides, fabric dyeing plants, electroplating plants, motor and power engineering plants, and battery and accumulator production plants [1,2]. Heavy metals flow into the ecosystem due to civilization and industrial development [3]. The creation of undefined mineral and organometallic linkages in aqueous and land environments can be attributed to heavy metals. In the environment, heavy metals show high mobility. Plant roots take up heavy metals which end up in the digestive systems of humans and animals [4]. Heavy metals pose serious threats to living organisms due to toxic effects on certain elements of the environment and bioaccumulation in the food chain [5]. The methods commonly used for metal ions removal are chemical precipitation, lime coagulation, ion exchange, reverse osmosis and solvent extraction from aqueous streams [6,7]. New technologies for removal of toxic metals from wastewaters have focused attention to biosorption, because biological materials have strong metal binding capacities. Adsorption technologies are of the most effective methods for dye removal due to its high efficiency, low cost, and easy to perform [8,9,10].

Several single solution experiments have been carried out on heavy metal removal [11,12,13], [14] used solid olive solid residues, [15,16,17] used activated sludge, biosorbents and aquatic macrophytes respectively for zinc removal from aqueous solutions. However, it is important to note that wastewaters contain various heavy

metals in solution [18,19,20]. It is prudent to carry out experimental work where one or more heavy metal is under study.

Biochar (BC) is prepared by pyrolysis (300°C and above) of a biomaterial in the absence of air until all the organic compounds except carbon are volatilised [21,22]. It has been used for tertiary treatment of municipal and industrial wastewaters [23]. Biochar adsorbs soluble organics namely nitrogen, sulphides and heavy metals in wastewater following biological or physical-chemical treatment [23]. Biochar though effective in adsorption, is limited to wastes with low organic concentrations (less than 5%), low inorganic concentrations (less than 1%) and unable to remove highly soluble organics, or those with low molecular weights [24,25]. To counter BC deficiencies in adsorption, there is need to activate it and enhance it with an oxide. Iron oxide has been used as an adsorbent in several studies in aqueous solutions [3,26,27,28]. However, to increase the number of adsorption sites, activated BC is among the adsorbents available for such studies [29,30,31].

The synthesis of activated biochar using microwaves is an area that needs more investigation because biochar generation from paper and pulp sludge has not received much research attention to date. Some researchers have reported an increase in surface area and porosity on microwave generated biochar, which was accompanied by an increase in the adsorption capacity of the adsorbent [32]. In addition, the smaller the particle size the greater the surface area for adsorption, so the activated BC ground to nano scale is expected to adsorb more [33].

Biochar adsorption studies have received a lot of attention from different angles. In agriculture, biochar has been employed in the remediation of soils from various forms of pollution [34]. Biochar has been found to be beneficial in reduction of soil atmospheric damage by soil wastes, removal of soil pollutants and improvement of soil quality. The adsorption capacities of biochar as an adsorbent on phosphorus and nitrogen have been investigated in agriculture [35]. It has been established that, the physicochemical properties of biochars are greatly influenced by feedstock material and the pyrolysis temperatures used [35,36].

In most cases the biosorption studies focused mainly on single solutions, few on binary solutions and very few on ternary solutions. An activated metal oxide biochar nano-composite represents an emerging group of adsorbents for removal of neutral and ionic contaminants in aqueous solutions [8]. This study focused on preparation of an activated metal oxide biochar nano-composite, characterisation and application in single solutions.

Activated BC has lower adsorption towards anions in solutions and it has been mainly applied to single solutions [29]. It needs modification for efficient removal of anions in single, binary and ternary solutions. A metal oxide biochar nano composite represent an emerging group of adsorbents for removal of neutral and ionic contaminants in aqueous solutions [8]. The main benefits of biosorption over conventional treatment methods are low cost and high efficiency. It also minimise chemical or biological sludge and the biosorbent can be regenerated [37,38]. The biosorption method has been proposed as an effective decolourization method for dye contaminated wastewaters [17,30,39,40]. Chemical methods for heavy metals removal are expensive. Engineered biochar (activated) has got unique properties potentially competent of heavy metal removal and decolourization ability in wastewater, therefore capable of removing dyes [17,28].

2. MATERIALS AND METHODS

2.1 Chemicals and Materials

The chemicals and materials which were used in this study includes Paper and Pulp Sludge (PPS), KOH analytical grade, HCL, iron chloride (FeCl₃), deionised water, pH meter (Mettler

Toledo), Shaker (Merck) and microwave (Samsung).

2.2 Preparation of Biochar (BC) and Fe₂O₃-BC

The BC and Fe₂O₃-BC were prepared according to the procedure mentioned by [32,41]. Briefly, 500 g of Paper and Pulp Sludge (PPS) obtained from Kadoma Paper Mills was dried at 105°C for 24hrs. The PPS was pre-ashed to remove volatiles in an oven at 200°C for 2hrs in an air tight container. The carbonization of the pre-ashed PPS was carried out in a muffle furnace at 500°C and 700°C separately for 2hrs. Potassium hydroxide (5 grams) was used to impregnate the biochar (1:2). Deionised water (100 mL) was added to dissolve all the KOH pellets, and the mixture left for 24 hrs at room temperature. Further activation of the impregnated BC was carried out using a microwave (800 watts) for 6 minutes. The sample was then cooled at room temperature and washed with hot distilled water. 12 grams of BC were thoroughly mixed with 4 grams of FeCl₃ solution. The mixtures were put in a muffle furnace at 500°C and 700°C separately for 2hrs each. The BC and Fe₂O₃-BC samples were ground, sieved through 250µm and stored in a closed container for use. The percentage conversion of PPS to BC was calculated as:

$$\%BC = \frac{m_2}{m_1} * 100$$

Where *m1* is the starting mass of PPS and *m2* is the mass of BC produced. The percentage conversion was 24% at 700°C

2.3 Characterisation of Biochar and Fe₂O₃-BC

The BC and Fe₂O₃-BC samples were characterised using Fourier transform infrared spectroscopy (FTIR), and scanning electron microscopy (SEM) for surface area analysis.

2.3.1 Fourier-transform infrared spectroscopy (FTIR)

Infrared red spectroscopy (FTIR 3000, WQF-520, attenuated) was used to identify the functional groups present in the synthesized samples of biochar before and after adsorption. The FT-IR studies were carried out in the 4000 to 400 cm⁻¹ wavenumber range. Background correction was done first and the dried solids were pressed with FTIR grade KBr and the pellets scanned 32

times using transmission mode with a resolution of 4 cm^{-1} .

2.4 Adsorption Studies

The adsorption properties of the synthesised $\text{Fe}_2\text{O}_3\text{-BC}$ and BC were determined by application in aqueous solutions of known heavy metal (Pb) and dye (Methyl Orange) concentrations. A UV/VIS Spectrophotometer (Lasany Double Beam LI-2802) and FAAS (AA-6701F) were used for the measurement of Methyl Orange and Lead concentrations. Three replicates of different concentrations were prepared one for lead removal and the other for methyl orange removal. 1000 ppm stock solutions each of Lead and Methyl orange were prepared in 1 litre distilled water. Afterwards, solutions were diluted to different concentrations. The pH values of solutions were adjusted by addition of HCl and NaOH. Effects of pH, contact time, adsorbent dosage and adsorbate concentration on the adsorption of Pb and Methyl Orange (MO) was investigated through a series of experiments.

2.4.1 Effect of pH

The effects of pH on adsorption of Pb were investigated at pH 2, 4, 10 and 12 using a 50 ml solution of 5 mg/L Pb, with 50 mg of $\text{Fe}_2\text{O}_3\text{-BC}$ and BC. For MO dye the effect of pH on adsorption were investigated at pH 2, 4, 8, 10 and 12 using a 20 ml of 50 mg/L MO solutions and 50 mg of $\text{Fe}_2\text{O}_3\text{-BC}$ and BC.

2.4.2 Effect of contact time

The effect of contact time on Pb adsorption was studied by shaking 50 mg of ($\text{Fe}_2\text{O}_3\text{-BC}$ and BC) for 15, 30, 60 and 90 minutes in a 50ml solution of 5 mg/L Pb. For MO, the effect of contact time was studied by shaking 50 mg of $\text{Fe}_2\text{O}_3\text{-BC}$ and BC for 15, 30, 60, and 90 minutes in a 20ml solution of 50 ppm MO solution.

2.4.3 Effect of adsorbate concentration

The effects of initial Pb concentration were studied using 5, 10, 15 and 20 mg/L of Pb solutions, for each adsorbent in and BC. The effect of initial dye concentration was studied using 50,100, 150, 200 and 250 mg/L MO solutions. The adsorbents for Pb and MO were 50 ml solution of 50 mg $\text{Fe}_2\text{O}_3\text{-BC}$ and 20 ml solution of 50 mg $\text{Fe}_2\text{O}_3\text{-BC}$ respectively.

2.4.4 Effect of adsorbent dosage

For Pb, the effect of adsorbent dosage was investigated by separately shaking a 50 ml solution of 5 mg/L of Pb with 50, 100, 150 and 200 mg $\text{Fe}_2\text{O}_3\text{-BC}$ for 30 minutes. The effect of adsorbent dosage on MO dye adsorption was investigated by separately shaking 50 mg/L solutions of MO dosage with 50, 100, 150, 200 and 250 mg $\text{Fe}_2\text{O}_3\text{-BC}$ for 30 minutes.

The initial and equilibrium concentrations of Pb^{2+} ions and MO in solutions were recorded and the amount adsorbed was calculated using the equations:

$$Q_e = \frac{V(C_i - C_e)}{m}$$

$$\% \text{ removal} = \frac{C_i - C_e}{C_i} * 100$$

Where C_i and C_e are the initial and equilibrium concentrations of Pb^{2+} ions and MO in ppm, Q_e is the amount of Pb^{2+} ions and MO adsorbed at equilibrium in mg/g, V is the volume of Pb^{2+} and MO solutions (L) and m is the mass of BC and $\text{Fe}_2\text{O}_3\text{-BC}$ in grams [10,40].

The Langmuir and Temkin equations were used to describe the equilibrium between the adsorbate and adsorbent represented as:

$$\frac{C_e}{Q_e} = \frac{C_e}{Q_{max}} + \frac{1}{Q_{max} * k_l}$$

$$Q_e = \frac{RT}{b} \ln a C_e$$

Where Q_{max} and k_l are the maximum adsorption capacity for the solid phase loading and the energy constant related to the heat of adsorption respectively. Plotting C_e/Q_e versus C_e , gives a straight line with Q_{max} and k_l determined from the intercept and the slope of the graph respectively. Also a plot of Q_e versus $\ln C_e$ gives a straight line [42].

3. RESULTS AND DISCUSSION

3.1 FTIR Characterisation

Fig. 1 shows $-\text{OH}$ stretching as can be depicted from the pronounced peaks in the range of $3300\text{-}3500 \text{ cm}^{-1}$. Also present were $-\text{CH}_x$ stretching bands, 1600 cm^{-1} related to the aromatic structure, 1390 cm^{-1} phenolics $-\text{OH}$, 830 cm^{-1} alkene CH band, 600 cm^{-1} due Fe-O bond and

490 cm^{-1} regions with $\text{Fe}_2\text{O}_3\text{-BC}$. The 490 cm^{-1} region with $\text{Fe}_2\text{O}_3\text{-BC}$ show the presence of Iron oxide. This is in agreement with literature [40]. The major differences between the peaks before adsorption and after adsorptions were where the 1100 cm^{-1} peak broadened to stretch from 9750-1275 cm^{-1} corresponding to the MO fingerprint region [43]. This indicates the effect of heavy metal and dye addition.

3.2 SEM Characterisation Results

The scanning electron microscopy (SEM) images above are showing the surface structures of the adsorbent materials. The surface area of both adsorbents was very large before adsorption experiments. After adsorption both biochars had reduced surface area.

3.3 Adsorption Experiment Results

3.3.1 Effect of pH

Fig. 3 shows that $\text{Fe}_2\text{O}_3\text{-BC}$ had a highest percentage MO removal of 89.81% at pH 2, while BC had 11.53% at pH 12. This may prove that at pH 2; Fe^{3+} is more effective in acidic conditions for the removal of MO. Fe^{3+} ions with the combination of H^+ ions present at low pH provided the much needed cationic binding sites for anion MO. Generally $\text{Fe}_2\text{O}_3\text{-BC}$ showed higher adsorption capacity for methyl orange at all pH values as compared to BC. The BC low adsorption may be attributed to the fact that it is a weak adsorbent towards anions. The trend depicts that $\text{Fe}_2\text{O}_3\text{-BC}$ is a better adsorbent for MO under any given pH conditions as compared to BC.

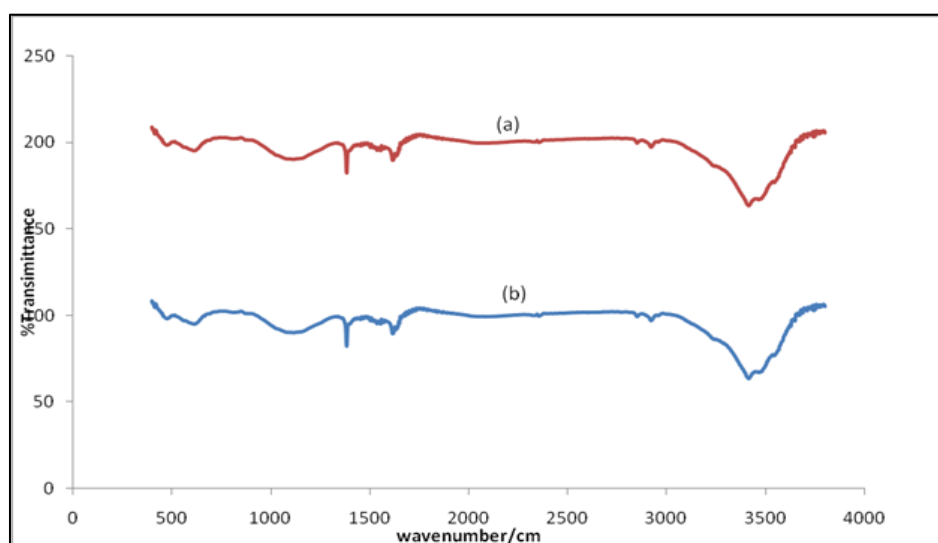


Fig. 1. $\text{Fe}_2\text{O}_3\text{-BC}$ FTIR spectra (a) after adsorption and (b) before adsorption

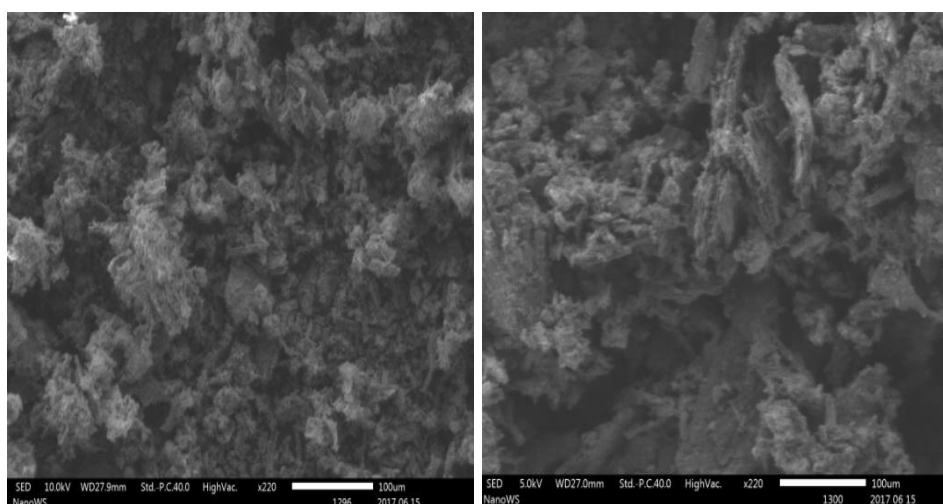


Fig. 2. SEM images for the Biochars

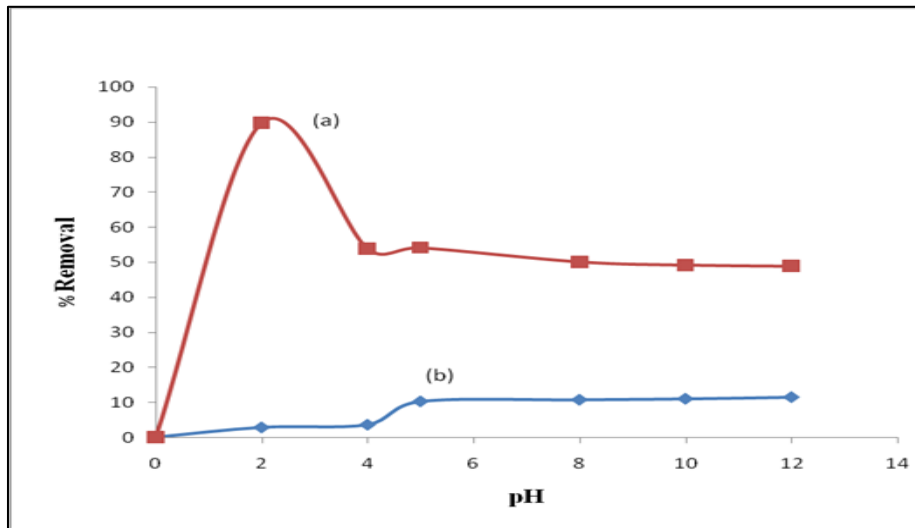


Fig. 3. Effect of pH on MO removal, (a) using Fe₂O₃-BC and (b) using BC

3.3.2 Effect of contact time

In Fig. 4, the high rate of MO removal (90%) was witnessed in the first 15 minutes. Less than 50% of MO was removed by BC after 90mins. The rapid MO adsorption is attributed to the presence of large number of surface sites initially and steadies thereafter [41]. The results clearly showed that Fe₂O₃-BC is a better adsorbent for methyl orange at any given contact time as compared to BC. This could be attributed to differences surface features and available surface areas among the adsorbents. It is also important to vary the particle size of the adsorbent to observe the trends in adsorption with various times.

Fig. 5 shows the effect of contact time on the adsorption of Pb²⁺.

Fig. 5 shows that both adsorbents BC and Fe₂O₃-BC had 97% Pb removal in the first 15 minutes. The adsorptions were rapid for the first 15 minutes and gradually approached equilibrium between 30 and 90 minutes. This trend ascertains that BC performs well with cations in adsorption studies. However, the adsorption performance of BC was found to be comparable to that of Fe₂O₃-BC on Pb²⁺ adsorption. The trend depicts that Fe₂O₃-BC performs well with both cations and non cations like methyl orange in adsorption.

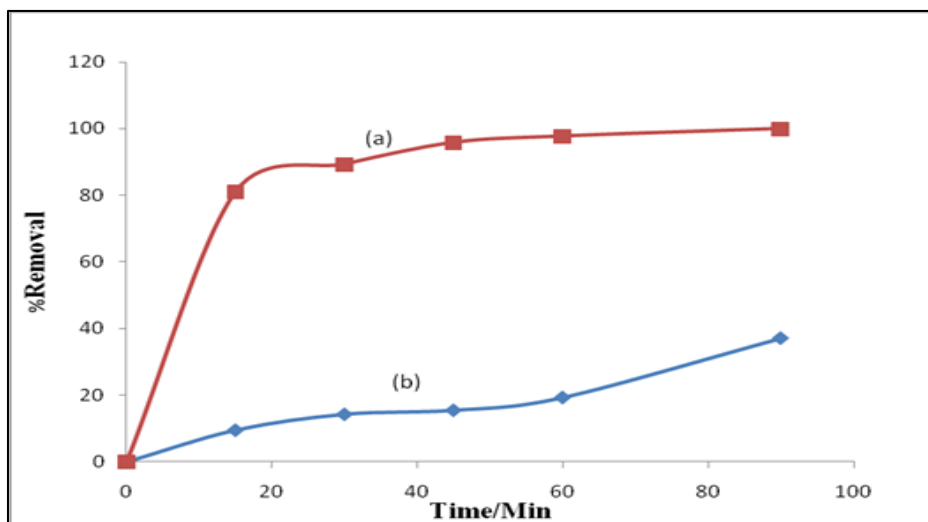


Fig. 4. Effect of contact time on MO removal, (a) using Fe₂O₃-BC and (b) using BC

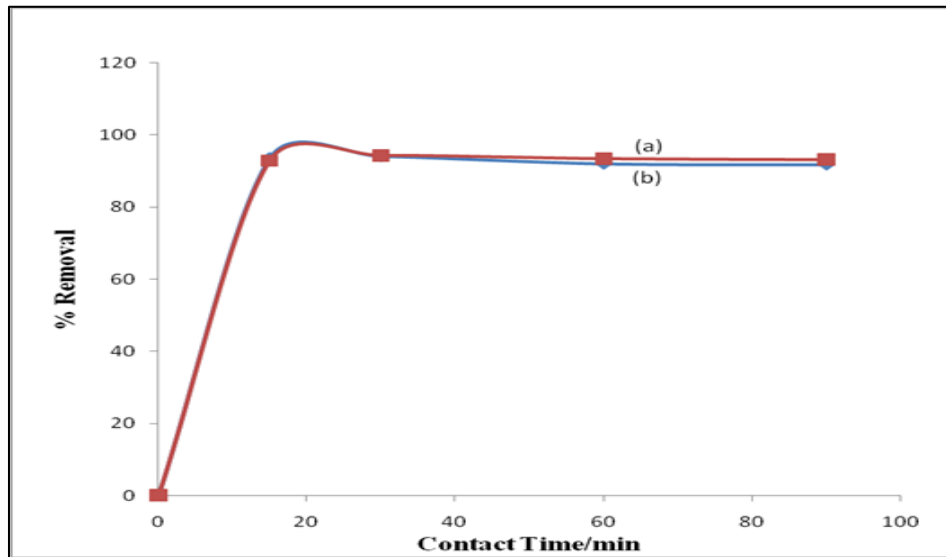


Fig. 5. Effect of contact time on Pb²⁺ removal (a) using Fe₂O₃-BC and (b) using BC

3.3.3 Effect of Adsorbate concentration

In Fig. 6, 91% MO removal was achieved after the addition of 70 mg/L adsorbate concentration for Fe₂O₃-BC. There were fluctuations in MO percentage removal as the concentration was increased. The BC adsorbent gave a maximum of 37% after the addition of 200 mg/L MO. The general decrease in percentage removal after addition of 75 mg/L adsorbate in both adsorbents could be because the active binding sites were all occupied as the MO concentration is increased. The graphs partially rise and levels off at very high adsorbate concentrations. Levelling off is attributed to saturation point, since only little

or no adsorptions are possible after saturation point.

Fig. 7 shows the optimum Pb²⁺ concentration of 6.5 mg/L for both adsorbents with 100% Pb²⁺ removal. The removal increased from 0 - 6.5 ppm. Both adsorbents show good sharp Pb²⁺ adsorptive properties at concentrations below 6.5 mg/L. There was little effect of concentration after 6.5 mg/L most probably due to saturation. Both adsorbents performed in almost a similar way, giving a maximum adsorption of 100%. There were no major differences in adsorption capacities of both adsorbents.

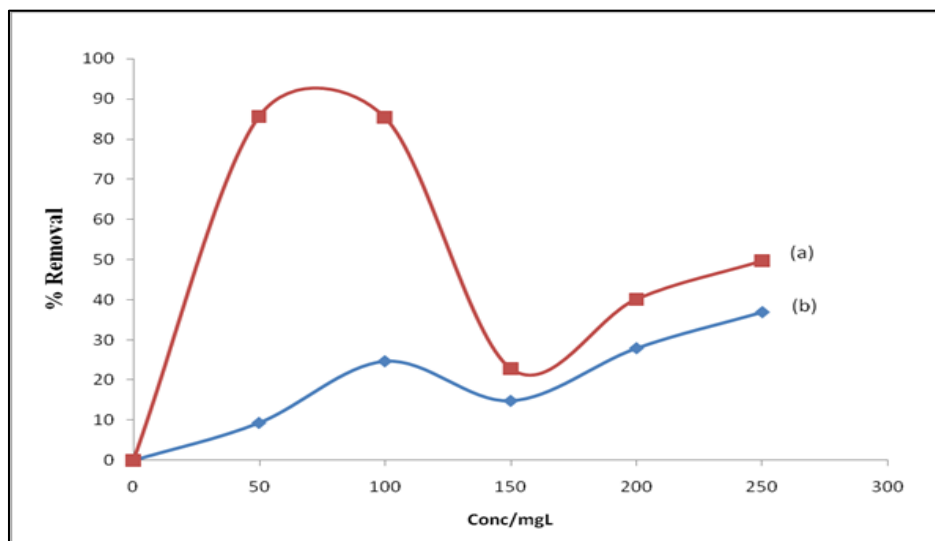


Fig. 6. Effect of adsorbate concentration on MO removal (a) using Fe₂O₃-BC and (b) using BC

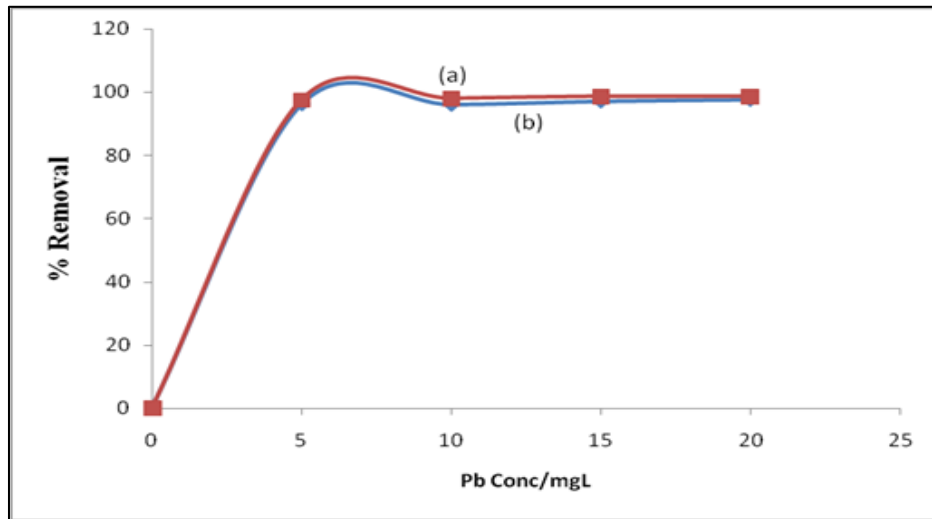


Fig. 7. Effect of adsorbate concentration on Pb²⁺ removal (a) using Fe₂O₃-BC and (b) using BC

3.3.4 Effect of Adsorbent dosage

In Fig. 8, 100 mg of Fe₂O₃-BC adsorbent had a 100% removal of MO. The BC adsorbent after addition of 250 mg had a maximum removal of 30.61% though there was a sharp increase between 200 and 250 mg. This is in agreement with literature that at low pH, BC has few H⁺ ions and at high pH more anions are predominantly present thereby hindering binding of MO onto the BC surface [30]. The Fe₂O₃-BC at low pH contained both Fe³⁺ and H⁺ ions which were available to adsorb the entire available MO in solution.

Fig. 9 shows that 100% of Pb²⁺ ions removal was achieved on addition of 65mg of both

adsorbents. There was rapid removal of Pb²⁺ ions from 0-65 mg, followed by a sharp decline towards 100 mg and 200 mg. There were no major differences in adsorption capacities of both the adsorbents. Adsorption diminishes as the active sites are used up.

3.4 Adsorption Isotherms

3.4.1 Langmuir Plots

Fig. 10 shows that the Langmuir isotherm and describes the adsorption of MO dye onto Fe₂O₃-BC with R² value of 0.999. The closeness of R² value to 1 indicates that the data obtained fits Langmuir Isotherm model of monolayer adsorption kinetics. The Fe₂O₃-BC nano-

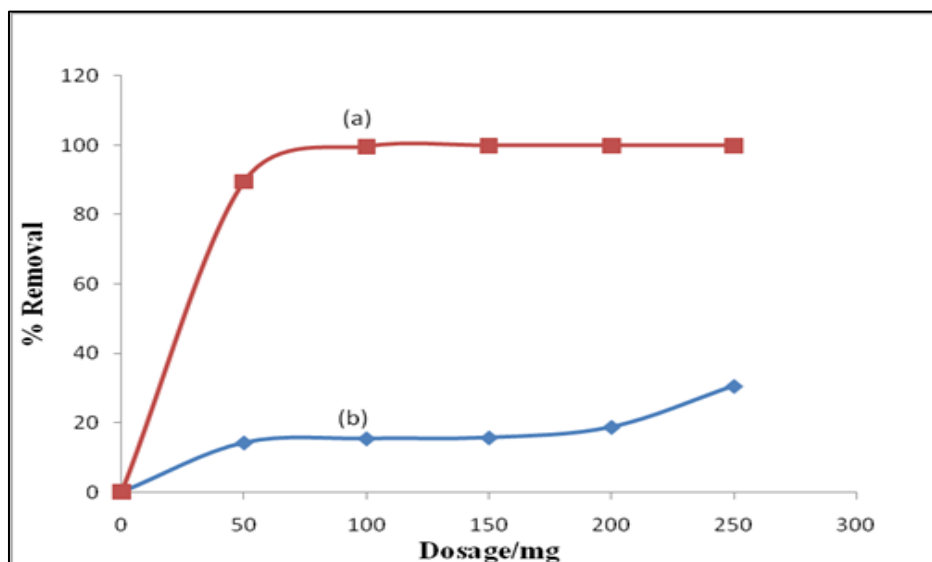


Fig. 8. Effect of adsorbent dosage on MO removal (a) using Fe₂O₃-BC and (b) using BC

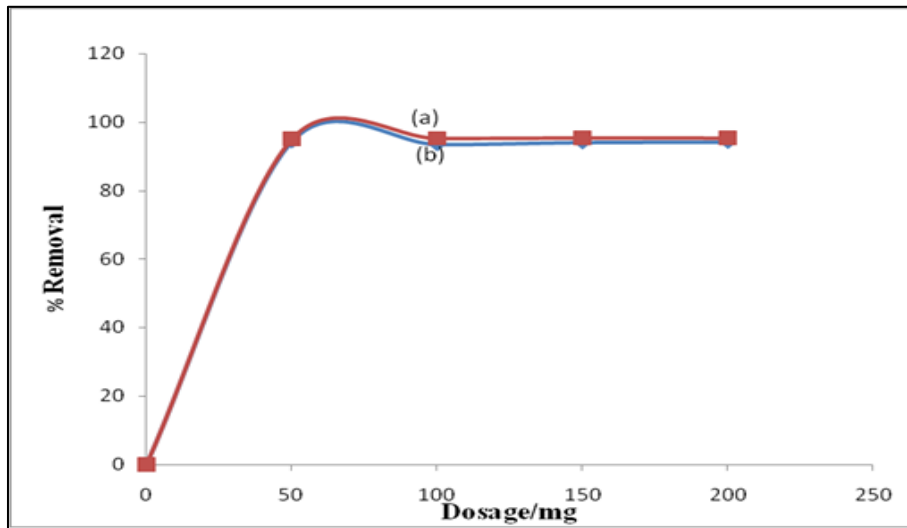


Fig. 9. Effect of Adsorbent dosage on Pb²⁺ removal (a) using Fe₂O₃-BC and (b) using BC

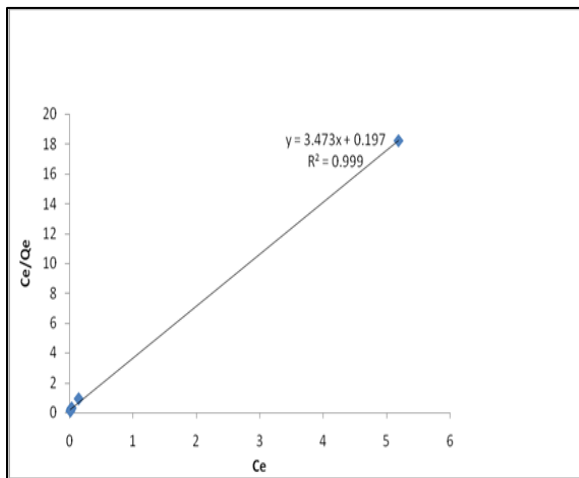


Fig. 10. Langmuir Plot for MO results

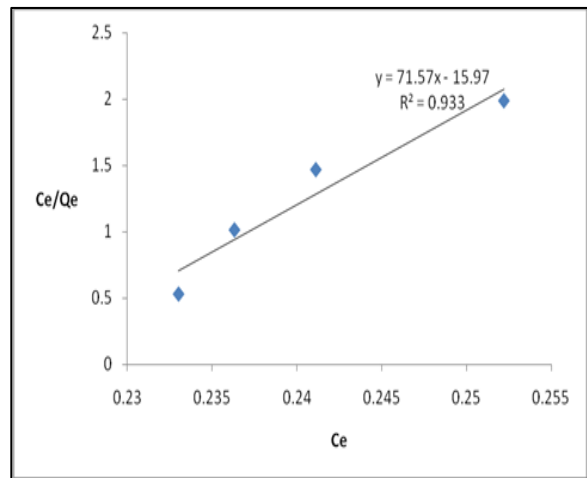


Fig. 11. Langmuir Plot for Pb²⁺ results

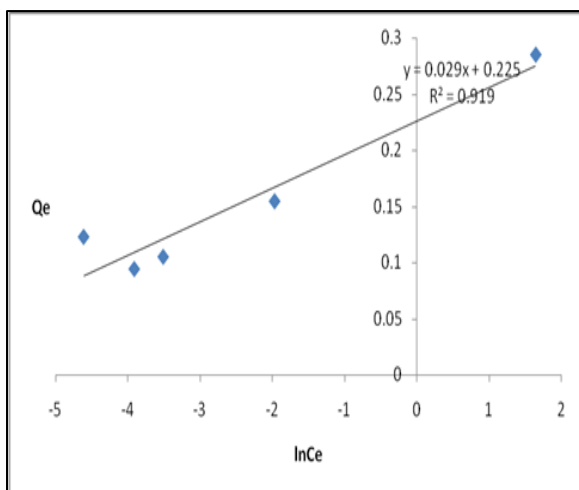


Fig. 12. Temkin Plot MO results

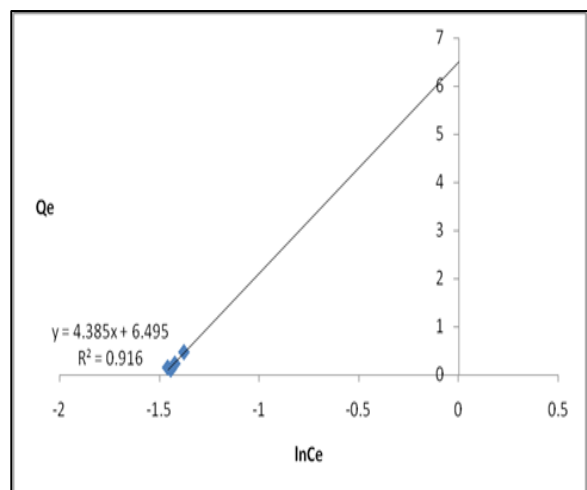


Fig. 13. Temkin Plot Pb²⁺ results

composite used can be said to have a series of distinct homogeneous sites available for binding the MO anions in solution. Fig. 11 describes the sorption of Pb^{2+} ions on the Fe_2O_3 -BC with R^2 value of 0.933 also fits the Langmuir Isotherm well.

3.4.2 Temkin plots

Fig. 12 and Fig. 13 show the Temkin plot with R^2 values of 0.919 and 0.916 for the sorption of MO onto Fe_2O_3 -BC and Pb^{2+} ions on the Fe_2O_3 -BC respectively, fitting in the model that the heat of adsorption of all the molecules in the layer would decrease linearly rather than logarithmic with coverage.

4. CONCLUSION

Fe_2O_3 -BC had highest percentage removal of 89.81% at pH 2 while BC had a highest of 11.55% at pH 12 of MO in solution. The dosage of 100 mg of Fe_2O_3 -BC had 100% removal of MO and 250 mg BC achieved 30.61% removal in 30 minutes. The maximum concentrations were 70 ppm and 55 ppm respectively for Fe_2O_3 -BC and BC adsorbents. In the removal of Pb^{2+} ions in solutions both Fe_2O_3 -BC and BC performances were almost similar with maximum removal of 97% in 30 minutes. 65 mg for both Fe_2O_3 -BC and BC adsorbents had 100% removal. The adsorption performance of Fe_2O_3 -BC is far much better than that of biochar in single aqueous solutions. Fe_2O_3 -BC is an effective alternative adsorbent for Pb^{2+} ions and methyl orange dye in aqueous solutions. There is need to perform further studies in order to find out the adsorption performance of Fe_2O_3 -BC in binary and ternary solutions. The adsorption performance of Fe_2O_3 -BC also needs to be evaluated on other common heavy metals and organic pollutants.

COMPETING INTERESTS

Authors have declared that no competing interests exist.

REFERENCES

1. Abbas SH, Ismail IM, Mostafa TM, Sulaymon AH. Biosorption of heavy metals: a review. *Journal of Chemical Science and Technology*. 2014;3(4):74-102.
2. Abdel-Ghani NT, El-Chaghaby GA. Biosorption for metal ions removal from aqueous solutions: A review of recent studies. *Int J Latest Res Sci Technol*. 2014;3(1):24-42.
3. Ahluwalia SS, Goyal D. Microbial and plant derived biomass for removal of heavy metals from wastewater. *Bioresource Technology*. 2007;98(12):2243-57.
4. Ahmad M, Rajapaksha AU, Lim JE, Zhang M, Bolan N, Mohan D, Vithanage M, Lee SS, Ok YS. Biochar as a sorbent for contaminant management in soil and water: A review. *Chemosphere*. 2014;1(99):19-33.
5. Al-Homaidan AA, Al-Houri HJ, Al-Hazzani AA, Elgaaly G, Moubayed NM. Biosorption of copper ions from aqueous solutions by *Spirulina platensis* biomass. *Arabian Journal of Chemistry*. 2014;7(1):57-62.
6. Alpat SK, Özbayrak Ö, Alpat Ş, Akçay H. The adsorption kinetics and removal of cationic dye, Toluidine Blue O, from aqueous solution with Turkish zeolite. *Journal of Hazardous Materials*. 2008;151(1):213-20.
7. Alslaibi TM, Abustan I, Ahmad MA, Foul AA. Comparison of activated carbon prepared from olive stones by microwave and conventional heating for iron (II), lead (II), and copper (II) removal from synthetic wastewater. *Environmental Progress & Sustainable Energy*. 2014;33(4):1074-85.
8. Baker MN, Taras MJ. *The quest for pure water: The history of the twentieth century*, volume 1 and 2. Denver: AWWA; 1981.
9. Beesley L, Marmiroli M. The immobilisation and retention of soluble arsenic, cadmium and zinc by biochar. *Environmental Pollution*. 2011;159(2):474-80.
10. Belaid KD, Kacha S, Kameche M, Derriche Z. Adsorption kinetics of some textile dyes onto granular activated carbon. *Journal of Environmental Chemical Engineering*. 2013;1(3):496-503.
11. Chaukura N, Murimba EC, Gwenzi W. Removal of Methyl Orange from Water using low-cost Biochar-Ferric Oxide Nanocomposites derived from Pulp and Paper Sludge. *Appl. Water Sci*; 2016.
12. Chen B, Chen Z, Lv S. A novel magnetic biochar efficiently sorbs organic pollutants and phosphate. *Bioresource Technology*. 2011;102(2):716-23.
13. Cortés-Martínez R, Martínez-Miranda V, Solache-Ríos M, García-Sosa I. Evaluation of natural and surfactant-modified zeolites in the removal of cadmium from aqueous solutions. *Separation Science and Technology*. 2004;39(11):2711-30.

14. Crittenden JC, Trussell RR, Hand DW, Howe KJ, Tchobanoglous G. MWH's water treatment: principles and design. John Wiley & Sons; 2012.
15. EPA, The history of drinking water treatment, Environmental Protection Agency, Office of Water (4606), Fact Sheet EPA-816-F-00-006, United States; 2000.
16. Goscianska J, Marciniak M, Pietrzak R. Mesoporous carbons modified with lanthanum (III) chloride for methyl orange adsorption. Chemical Engineering Journal. 2014;1(247):258-64.
17. Hamdaoui O. Batch study of liquid-phase adsorption of methylene blue using cedar sawdust and crushed brick. Journal of hazardous materials. 2006;135(1-3):264-73.
18. Hammaini A, González F, Ballester A, Blázquez ML, Munoz JA. Simultaneous uptake of metals by activated sludge. Minerals Engineering. 2003;16(8):723-9.
19. Huang H, Cao L, Wan Y, Zhang R, Wang W. Biosorption behavior and mechanism of heavy metals by the fruiting body of jelly fungus (*Auricularia polytricha*) from aqueous solutions. Applied microbiology and biotechnology. 2012;96(3):829-40.
20. Huang S, Lin G. Biosorption of Hg (II) and Cu (II) by biomass of dried *Sargassum fusiforme* in aquatic solution. Journal of Environmental Health Science and Engineering. 2015;13(1):21.
21. Kumar S, Loganathan VA, Gupta RB, Barnett MO. An assessment of U (VI) removal from groundwater using biochar produced from hydrothermal carbonization. Journal of environmental management. 2011;92(10):2504-12.
22. Mašek O, Budarin V, Gronnow M, Crombie K, Brownsort P, Fitzpatrick E, Hurst P. Microwave and slow pyrolysis biochar—Comparison of physical and functional properties. Journal of Analytical and Applied Pyrolysis. 2013;1(100):41-8.
23. Mckay G, Allen SJ. Surface mass transfer processes using peat as an adsorbent for dyestuffs. The Canadian Journal of Chemical Engineering. 1980;58(4):521-6.
24. Motasemi F, Afzal MT. A review on the microwave-assisted pyrolysis technique. Renewable and Sustainable Energy Reviews. 2013;1(28):317-30.
25. Mukherjee A, Zimmerman AR, Harris W. Surface chemistry variations among a series of laboratory-produced biochars. Geoderma. 2011;163(3-4):247-55.
26. Norton L, Baskaran K, McKenzie T. Biosorption of zinc from aqueous solutions using biosolids. Advances in Environmental Research. 2004;8(3-4):629-35.
27. Outwater A. Water—A Natural History. New York: Basic Book, a division of Harper Collins Publisher; 1996.
28. Pagnanelli F, Toro L, Veglio F. Olive mill solid residues as heavy metal sorbent material: a preliminary study. Waste Management. 2002;22(8):901-7.
29. Pandey S, Mishra SB. Sol-gel derived organic-inorganic hybrid materials: Synthesis, characterizations and applications. Journal of Solgel Science and Technology. 2011;59(1):73-94.
30. Pereira MF, Soares SF, Órfão JJ, Figueiredo JL. Adsorption of dyes on activated carbons: influence of surface chemical groups. Carbon. 2003;41(4):811-21.
31. Rich G, Cherry K. Hazardous Waste Treatment Technology, Pudvan Publ. Co., New York; 1987.
32. Shi B, Li G, Wang D, Feng C, Tang H. Removal of direct dyes by coagulation: The performance of preformed polymeric aluminum species. Journal of hazardous materials. 2007;8(143):567-74.
33. Siculus, Diodorus. Library of History, Loeb Classical Library. 1939;III.
34. Wang J, Chen C. Biosorbents for heavy metals removal and their future. Biotechnology advances. 2009;27(2):195-226.
35. Wang S, Gao B, Zimmerman AR, Li Y, Ma L, Harris WG, Migliaccio KW. Removal of arsenic by magnetic biochar prepared from pinewood and natural hematite. Bioresource technology. 2015;1(175):391-5.
36. Yao Y, Gao B, Chen J, Zhang M, Inyang M, Li Y, Alva A, Yang L. Engineered carbon (biochar) prepared by direct pyrolysis of Mg-accumulated tomato tissues: characterization and phosphate removal potential. Bioresource technology. 2013;1(138):8-13.
37. Zhang M, Gao B, Varnoosfaderani S, Hebard A, Yao Y, Inyang M. Preparation and characterization of a novel magnetic biochar for arsenic removal. Bioresource technology. 2013;1(130):457-62.
38. Zhang M, Gao B. Removal of arsenic, methylene blue, and phosphate by biochar/AlOOHnanocomposite. Chemical Engineering Journal. 2013;15(226):286-92.

39. Zhou Y, Gao B, Zimmerman AR, Chen H, Zhang M, Cao X. Biochar-supported zerovalent iron for removal of various contaminants from aqueous solutions. *Bioresource Technology*. 2014;1(152):538-42.
40. Zhou Y, Gao B, Zimmerman AR, Fang J, Sun Y, Cao X. Sorption of heavy metals on chitosan-modified biochars and its biological effects. *Chemical Engineering Journal*. 2013;1(231):512-8.
41. Zhu D, Kwon S, Pignatello JJ. Adsorption of single-ring organic compounds to wood charcoals prepared under different thermochemical conditions. *Environmental Science & Technology*. 2005;39(11):3990-8.
42. Yang X, Zhang S, Ju M, Liu L. Preparation and modification of biochar materials and their application in soil remediation. *Applied Sciences*. 2019;9(7):1-25.
43. Zhou L, Xu D, Li Y, Pan Q, Wang J, Xue L, Howard A. Phosphorus and nitrogen adsorption capacities of biochars derived from feedstocks at different pyrolysis temperatures. *Water*. 2019;11(8):1-16.

© 2019 Shumba et al.; This is an Open Access article distributed under the terms of the Creative Commons Attribution License (<http://creativecommons.org/licenses/by/4.0>), which permits unrestricted use, distribution, and reproduction in any medium, provided the original work is properly cited.

Peer-review history:

The peer review history for this paper can be accessed here:

<http://www.sdiarticle4.com/review-history/52734>